



HAL
open science

Molecular dynamics study of water in contact with TiO₂ rutile-110, 100, 101, 001 and anatase-101, 001 surface

Ritwik Kavathekar, Pratibha Dev, Niall J English, Don Macelroy

► **To cite this version:**

Ritwik Kavathekar, Pratibha Dev, Niall J English, Don Macelroy. Molecular dynamics study of water in contact with TiO₂ rutile-110, 100, 101, 001 and anatase-101, 001 surface. *Molecular Physics*, 2011, pp.1. <10.1080/00268976.2011.582051>. <hal-00701867>

HAL Id: hal-00701867

<https://hal.science/hal-00701867v1>

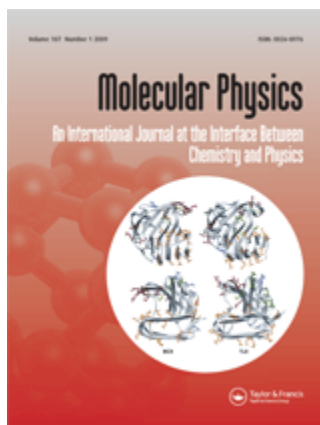
Submitted on 27 May 2012

HAL is a multi-disciplinary open access archive for the deposit and dissemination of scientific research documents, whether they are published or not. The documents may come from teaching and research institutions in France or abroad, or from public or private research centers.

L'archive ouverte pluridisciplinaire **HAL**, est destinée au dépôt et à la diffusion de documents scientifiques de niveau recherche, publiés ou non, émanant des établissements d'enseignement et de recherche français ou étrangers, des laboratoires publics ou privés.



HAL Authorization



Molecular dynamics study of water in contact with TiO₂ rutile-110, 100, 101, 001 and anatase-101, 001 surface

Journal:	<i>Molecular Physics</i>
Manuscript ID:	TMPH-2011-0075.R1
Manuscript Type:	Full Paper
Date Submitted by the Author:	08-Apr-2011
Complete List of Authors:	Kavathekar, Ritwik; UCD Dev, Pratibha; UCD English, Niall; UCD MacElroy, Don; UCD
Keywords:	molecular dynamics, TiO ₂ surface, oxide-water interface, rutile, anatase

SCHOLARONE™
Manuscripts

RESEARCH ARTICLE

Molecular dynamics study of water in contact with TiO₂ rutile-110, 100, 101, 001 and anatase-101, 001 surfaceRitwik S. Kavathekar ^a, Pratibha Dev ^a, Niall J. English ^{a*} and J.M.D. MacElroy ^a

^a *The SFI Strategic Research Cluster in Solar Energy Conversion and the Centre for Synthesis and Chemical Biology, School of Chemical and Bioprocess Engineering, University College Dublin, Belfield, Dublin 4, Ireland.*

* Corresponding author:

Dr Niall English,
School of Chemical and Bioprocess Engineering,
University College Dublin,
Belfield, Dublin 4, Ireland.
niall.english@ucd.ie
Phone: +353(1)716 1646

Molecular dynamics study of water in contact with TiO₂ rutile-110, 100, 101, 001 and anatase-101, 001 surface

We have carried out classical molecular dynamics of various surfaces of TiO₂ with its interface with water. We report the geometrical features of the first and second monolayers of water using a Matsui Akaogi (MA) force field for the TiO₂ surface and a flexible single point charge model for the water molecules. We show that the MA force field can be applied to surfaces other than Rutile-(110). It was found that water OH bond lengths, H-O-H bond angles and dipole moments do not vary due to the nature of the surface. However, their orientation within the first and second monolayers suggest that planar Rutile-(001) and Anatase-(001) surfaces may play an important role in not hindering removal of the products formed on these surfaces. Also, we discuss the effect of surface termination in order to explain the layering of water molecules throughout the simulation box.

Keywords: molecular dynamics, TiO₂ surface, oxide-water interface, rutile, anatase

1. Introduction

Titanium dioxide (TiO₂) surfaces have been of most interest for photochemical degradation of organic compounds as bactericides, hydrophobic coatings, [1] and show considerable potential in the field of solar energy conversion by mediation of photocatalytic splitting of water, as demonstrated by the Fujishma-Honda reaction [2]. This reaction is a four-hole mechanism, [3] producing O₂/H₂ gas, and takes place in the presence of solar radiation and in the absence of external bias. Electron-hole pairs are generated in the bulk and migrate towards the surface where the hole reacts with water. Although several materials have been used as photocatalysts for H₂/O₂ production, like nanoribbons of CdSe-MoS₂, [4] core (GaN:ZnO)-shell (Cr₂O₃), [5] oxynitrides, [6] BiVO on reduced graphene, [7] phosphate-based Co²⁺ catalysts, [8] algae, [9] and, more recently, Fe₂O₃, [10] TiO₂ remains a strong contender due to its stability, cost-effectiveness and non-toxicity. It is clear that the structure of TiO₂-water interface plays a great role in enhancing efficiency of photolysis. Rutile is the most abundant polymorph of TiO₂ and the (110) face is the most stable surface. The pristine (110) surface is inert but water splitting takes place at defect sites [11] created by oxygen vacancies, and much experimental [12] and theoretical [13-

1
2
3 16] scrutiny has been directed consequently thereto. Water molecules may undergo dissociative
4 or molecular adsorption, or both [1]. One of the early calculations [17] proposing mixed water
5 adsorption modes was by Lindan *et.al*, based on a first-principles approach. Quasi-elastic
6 neutron scattering (QENS) studies along with molecular dynamics (MD) [18] have demonstrated
7 that water molecules form hydrogen-bonded second and third layers above the (110) surface.
8 Back-scattering neutron spectroscopy reports, [19] supported by MD, show that, on average,
9 participation of water molecules in four hydrogen bonds is needed for slow dynamical
10 (“Arrhenius type”) behaviour, while that dynamics (“non-Arrhenius type”) is possible if less than
11 three hydrogen bonds are present, depending on the level of hydration. Most of the reported
12 work [15,16,20] on water adsorption on rutile-(110) deals with adsorption isotherm prediction,
13 surface charging effects using the multisite complexation model (MUSIC) and correlating
14 behaviour with pH titration employing both classical and quantum chemical approaches. Density
15 functional theory using plane-augmented wave potentials have been used [15] to model
16 photooxidation of water with detailed energetic analysis. Also some solvation studies of TiO₂
17 surfaces using reaction fields and conductor-like, screening models for real solvents (COSMO-
18 RS) have been reported [16] for predicting proton affinity to the surface. Another important
19 rutile surface is (100), which, along with (110), contributes to the reaction mechanism of
20 photocatalytic water-splitting. *Ab initio* simulations based on Car-Parrinello Molecular Dynamics
21 (CPMD) on perfect and defect rutile-(110) and rutile-(100) surfaces [21] resulted only in weakly
22 stabilized H₂O molecule on the pristine surface. But OH dissociation was observed on defects
23 (creation of an oxygen vacancy) rutile-(100) surface and not on the perfect or defect rutile-(110)
24 as postulated. Rutile (101) contributes to about 20% of the bulk surface, along with rutile-(100),
25 and thus these constitute particularly important surfaces for water absorption. Although most
26
27
28
29
30
31
32
33
34
35
36
37
38
39
40
41
42
43
44
45
46
47
48
49
50
51
52
53
54
55
56
57
58
59
60

1
2
3 studies have been performed using quantum methods, classical dynamics remains an important
4
5 tool for studying larger picosecond time scale phenomenon with macroscopically observed
6
7 properties.
8
9

10 11 **2. Simulation Methodology**

12 Anhydrous rutile-(110), (100), (101), (001) and anatase-(101), (001) surface geometries were
13 realised in slab configurations in the x - y plane and **water molecules added** in the z -direction for at
14
15 least 50 Å distance. The respective molecular compositions and structural details for relaxed
16
17 water-titania interfaces are specified in Table I. [Insert Table 1 near here] Classical molecular
18
19 dynamics was performed in the NVT ensemble at 300 K using DL_POLY [22] in conjunction
20
21 with a Nosé-Hoover thermostat, the **three-dimensional** Ewald summation for long-range
22
23 electrostatic interactions **with a relative precision within 10^{-5}** and the Velocity-Verlet scheme
24
25 with a time step of 1 fs. All production simulations were run for 1 ns after 200 ps of
26
27 equilibration. **All simulations were periodic in three dimensions.** We used the force field as
28
29 reported by Bandura *et.al.* [14] and Predota *et.al.* [20] for all surfaces and the water model and
30
31 cross interaction parameters are summarised in Table II. [Insert Table near here] For the crystal,
32
33 the Matsui and Akaogi (MA) [23] parameters were used, while water was represented by a
34
35 Lennard-Jones potential with a harmonic $H_w-O_w-H_w$ angle potential and a Morse-stretch O_w-H_w
36
37 bond potential. Water bond angles and bond lengths were not constrained and thus a flexible
38
39 SPC model was used. **Using a classical Morse stretching potential enables one to follow bond-**
40
41 **length changes during the course of the simulation. This, however, is a non-dissociative model**
42
43 **and is thus unable to reproduce water splitting or OH dissociation. In the present work, we are**
44
45 **interested primarily in the orientation and detection of any strain on the water molecules within**
46
47 **the monolayers.** The entire TiO_2 block was mobile for all surfaces throughout the simulation.
48
49
50
51
52
53
54
55
56
57
58
59
60

1
2
3 Bulk rutile is defined by lattice vectors of length $a_0=b_0= 4.593 \text{ \AA}$, $c_0=2.959 \text{ \AA}$ with symmetry
4 group *P42/MNM*. Bulk anatase has lattice vectors $a_0=b_0= 3.776 \text{ \AA}$ and $c_0=9.486 \text{ \AA}$ and a
5
6 symmetry group *I41/AMD*. All surfaces were constructed by cleaving super cells made from bulk
7
8 crystals. The rutile-(110) surface (Fig. 1A) is the most thermodynamically stable and constitutes
9
10 a major part of the bulk TiO_2 surface. [Insert Figure 1 near here] The (110) surface was
11
12 reconstructed for charge auto-compensation [1]. The rutile (110) oxygen-terminated surface is
13
14 non-polar [24] and hence a dipole-free surface was ensured. The rutile (110) surface consists of
15
16 bridging oxygen atoms bonded to 6-coordinated titania (Ti_{6c}) and a 3-coordinated oxygen (O_{3c})
17
18 bonded to Ti_{5c} and Ti_{6c} atoms. These Ti_{5c} surface atoms were used as the plane against which
19
20 height measurements of water oxygen (O_w) atoms were made. Surface termination produces
21
22 coordinatively unsaturated –sites (CUS), which differ in charge from the bulk. Although surface-
23
24 modified charges are available [14] for the rutile (110) surface, they have not been specified for
25
26 other surfaces, to the best of the authors' knowledge. The rutile (100) surface (Fig. 1(B))
27
28 constitutes about 20% of the bulk rutile and has a ridge pattern created by 2-coordinated bridging
29
30 oxygen atoms connected to Ti_{5c} . The rutile (100) surface is similar to that of rutile (110), except
31
32 that the bridging plane of $\text{Ti}_{5c}\text{-O}_b\text{-Ti}_{5c}$ is inclined at an angle, rather than perpendicular as in
33
34 (110). The rutile (101) plane (Fig 1(C)) is similar to that of rutile (100) and also composes 20%
35
36 of naturally occurring rutile. It is also composed of Ti_{5c} and O_{2c} structures, but the Ti_{5c} bond
37
38 length differs to the O_{2c} creating two different types of O_{2c} . Also, the rutile (101) plane is tilted
39
40 with respect to the z -direction (chosen as the standard orientation for solvation, as mentioned
41
42 previously), and was rotated for alignment vis-à-vis the z -direction. The rutile-(001) surface (Fig.
43
44 1(D)) forms a lesser part of naturally occurring rutile, and although only a few experiments have
45
46 been performed on this surface, it was considered in this study for the sake of completeness and
47
48
49
50
51
52
53
54
55
56
57
58
59
60

1
2
3 comparison. The rutile-(001) surface has 4-coordinated Ti atoms (Ti_{4c}) bonded to O_{2c} atoms,
4
5 along with alternating Ti_{6c} atoms bonded to O_{2c} atoms, giving it a corrugated, ridge-like
6
7 structure. This surface is comparatively more acidic due to large-coordinate unsaturation (CUS)
8
9 of Ti_{4c} atoms. It is also unstable and hence difficult to experimentally study due to spontaneous
10
11 reconstruction of the surface.
12
13

14
15 Anatase is the more photoactive polymorph and is also proposed [25] to be an efficient candidate
16
17 for photoelectrolysis of water. It is also used in other solar energy-based applications like dye
18
19 sensitized solar cells, and therefore the water-anatase interface constitutes an important system
20
21 for comparative studies vis-à-vis rutile. The anatase (101) surface (Fig 2(A)) exhibits a terrace-
22
23 like structure formed by fully-coordinated Ti_{6c} atoms bonded to O_{3c} atoms and under-coordinated
24
25 Ti_{5c} with O_{2c} . [Insert Figure 2 near here] The surface is tilted at an angle with respect to the [101]
26
27 direction and was rotated to align with the z -axis, *i.e.*, [001]. Although the pristine anatase (101)
28
29 surface is inert to photolysis, some reports have indicated dissociative adsorption onto anatase-
30
31 (001) surfaces [25]. The anatase-(001) face is not stable, and various instances of this have been
32
33 reported [1]. Anatase-(001) (Fig 2(B)) has a flat plane connected by alternating rows of Ti_{5c} and
34
35 O_{2c} atoms in a three- and two-fold manner, respectively. Surfaces can be made non-polar [24] by
36
37 varying the surface termination. This surface dipole effect was manifested in our simulations
38
39 wherein water was found to layer on top of such dipole “not-free” surfaces.
40
41
42
43
44
45

46 47 **3. Results and Discussion**

48 The density distributions, based on the distance of the water oxygen (O_w) atoms from the crystal
49
50 plane, are depicted in Fig. 3. [insert Figure 3 near here] The density of water was calculated as
51
52 the mass of number of water molecules per 0.1 \AA volume increment away from the surface
53
54 (counting a molecule present if its O_w is in each grid-element), *i.e.*, along the direction of
55
56
57
58
59
60

1
2
3 heterogeneity (the z -direction). This density profile was used as a guide to sample respective
4 properties in consecutive layers. Fig. 3a shows the order of distance to the rutile plane is (100) <
5 (101) < (110) = (001). The plane used for calculation of the distance to O_w atoms was taken to be
6 the first Ti plane found on the surface. The distance for rutile-(100) is found to be 1.9 Å, due to
7 the (electrostatic) attraction of Ti_{5c} atoms below the O_{2c} to the water oxygen atoms. This is
8 similar to the (101)-case, for which the first exposed plane is formed by O_{2c} atoms, but the Ti_{5c}
9 atoms are bonded to the O_{2c} atoms in the same plane, and hence the water oxygen atoms are at
10 approximately 2.3 Å distance due to O_{2c} - O_w repulsion compensated by Ti_{5c} - O_{2c} attraction. The
11 (110)-surface plane was taken to be that formed by Ti_{5c} rather than the bridging oxygen atoms.
12 Water molecules occupy the spaces in between the Ti_{5c} (probably owing to the tetrahedral water
13 geometry formed by two hydrogen atoms and two lone pairs), rather than on top of it. For the
14 (001) surface, alternated with O_{2c} and Ti_{4c} sites, the H_w are therefore tilted towards the O_{2c}
15 atoms, creating a tilt angle and 'pulling' the water molecule inwards. For anatase surfaces, the
16 order of distance to the plane is in the order (101) < (001). The (101) ridged, terrace-like
17 structure permits the water molecules to remain in-between the O_{2c} atoms, binding more weakly
18 to the Ti_{5c} surface atoms, whilst remaining hydrogen-bonded to O_{2c} atoms. The anatase-(001),
19 planar surface creates a flat monolayer, at a distance of 2.5 Å. Previous calculations using similar
20 force fields have been reported [20] and references therein. However these simulations [20] were
21 performed on stationary surfaces derived from quantum simulations with a rigid SPC water
22 model, 3D Ewald sum with correction for 2D periodic geometry electrostatics at 298.15 K
23 temperature. They reported a z axis density profile distance for water oxygens at 2.2 Å for
24 neutral rutile-(110) surface. CPMD simulations [26] for anatase-(101) and (001) surfaces showed
25 dissociative adsorption of water molecules on anatase-(001). The Ti_{5c} - O_w (dissociated water)
26
27
28
29
30
31
32
33
34
35
36
37
38
39
40
41
42
43
44
45
46
47
48
49
50
51
52
53
54
55
56
57
58
59
60

1
2
3 distance was reported 1.84 Å and $Ti_{5c}-O_w$ (molecular water) observed at 2.14. They observed no
4 dissociation on pristine anatase-(101). [Insert Figure 4 and 5 near here]
5
6

7
8 In order to investigate intramolecular strain in the water molecules at the interface we calculated
9 as depicted Figs. 4 and 5 respectively the probability distributions of water ($H_w-O_w-H_w$) angles
10 and O_w-H_w bond lengths in the adsorbed monolayer (evident from the density profiles of Fig. 3,
11 and labeled as 'L1'). However no significant shifts were found for interfacial, adsorbed water
12 molecules relative to bulk water molecules. The average bond angle in the adsorbed layer was
13 106.11° compared to 107.22° in the bulk for the rutile-(101) case, while for the anatase-(101)
14 case, the adsorbed layer's angle was 105.55° compared to 106.66° in the bulk liquid. Also the
15 O_w-H_w bond length showed no significant deviation L1 and bulk, with the average bond length
16 (Fig. 5) being 1.02 Å. This geometry is close to the values of 108.5° and 0.98 Å for the water
17 angle and bond length respectively, reported [27] by plane wave based *ab initio* DFT using GGA
18 functional on rutile-(110) surface, which were modeled for STM experiments. [Insert Figure 7
19 near here]
20
21
22
23
24
25
26
27
28
29
30
31
32
33
34
35

36 We calculated distribution profiles for molecular dipole moment of water (Fig. 6) in L1 and
37 found its average value to be at 2.4 D, without significant deviation from the other layers and is
38 consistent with the value of condensed water [28] at all interfaces. This is consistent with water
39 bond angles and bond lengths in all the simulations. [Insert Figure 7 near here] Figure 7 shows
40 angle made by a vector on the titania surface and the molecular dipole moment vector of water. It
41 is seen that at the rutile-(110)-water interface, dipole vector points downwards making a 90°
42 angle with the surface. However, for rutile-(001) and anatase-(001) surfaces, the vectors are
43 pointed along the surface on either side. Water dipole vectors at the rutile-(100) surface are
44 oriented in one direction along the surface while, for rutile-(101) water dipole vectors are
45
46
47
48
49
50
51
52
53
54
55
56
57
58
59
60

1
2
3 pointing towards and along the surface. Sampling between the regions within 5 Å of the interface
4
5 involves at least two water monolayers, as seen in Figs. 3. Calculating water dipole moment
6
7 vectors at these monolayer distances resolves the orientation more clearly, as shown in Fig 8.
8
9 Rutile-(110) (Fig. 8(A)) distinguishes between the first and second monolayer (ML) dipole
10
11 vector orientations of water at distance of 2.4 Å and 3.9 Å respectively. [Insert Figure 8 near
12
13 here] The first ML water molecules are oriented perpendicular to the surface as depicted in Fig
14
15 1A (black/dark shade) and the second ML (yellow/light shade) dipole moment vectors to be
16
17 pointing along either sides of the surface. Water molecules in both the monolayers are stabilized
18
19 by hydrogen bonding with bridging oxygens' of rutile-(110). Rutile-(100) face has a slanting
20
21 roof-like structure with bridging oxygens' at the edges: hence their angles are off to one side
22
23 along the surface (Fig 1(B)), with first ML and second ML waters appearing at distances of 1.9
24
25 Å and 3.1 Å respectively. The first ML and second ML for rutile-(101) appear at 2.3 Å and 3.6 Å
26
27 with a spread of angles in the second ML and a partial orientation in the first ML, owing to the
28
29 serrated nature of the surface. The second ML waters have H_w atoms bonding with bridging
30
31 oxygens' with O_w pointing opposite to the z-direction and the first ML waters are spread in a
32
33 perpendicular direction with O_w pointing towards Ti_{5c}. The rutile-(001) surface is planar,
34
35 wherein Ti_{4c} atoms are sandwiched between O_{2c} competing with H-bonding with water
36
37 molecules, giving them an angular orientation with O_w pointing towards Ti_{4c}. This pushes the
38
39 second ML away to 5.2 Å from the first ML at 2.4 Å. A small shoulder at 2.8 Å in the density
40
41 distribution of rutile-(001) (Fig. 3(A)) indicates a second orientation within the first ML with H_w
42
43 pointing towards O_{2c} atoms. The anatase-(101) surface is similar to rutile-(100) except that Ti
44
45 and O layers alternate in the x-direction hence their angles are similar, *i.e.*, along the surfaces.
46
47 The anatase-(101) first ML and second ML occur at 2.4 Å and 3.8 Å respectively. Anatase-(001),
48
49
50
51
52
53
54
55
56
57
58
59
60

1
2
3 like the rutile-(001) is a planar surface but much flatter without any “cavities”, thus creating a
4 denser and uniform first and second monolayers. The anatase-(001) first and second ML are at
5
6 2.9 Å and 5.7 Å respectively.
7
8
9

10 11 **4. Conclusions**

12 We have performed classical molecular dynamics of rutile (110), (101), (001), (001) and anatase
13 (101), (001) faces for polymorphs of TiO₂ in contact with water, using a flexible Morse potential
14 for water and Matsui-Akaogi potential for the crystal, wherein the entire crystal block is mobile
15 and not fixed/constrained. **Newer force field models employing polarisation effects, as recently**
16 **suggested by Han *et.al.* [29], would perhaps be a good approach to model the flexible lattice; in**
17 **this case [29], phonon dispersion curves were fitted with *ab initio* density functional theory**
18 **(LDA) to the classical force field model.** The orientation of water molecules depends heavily on
19 the surface terminations of either side of the solid surfaces. Analysis of the distribution profiles
20 of O_wH_w bond lengths and H_w-O_w-H_w angles show no considerable shift from their equilibrium
21 values along the sampled layers. The orientation of water molecules in the first and second
22 monolayer is considerably influenced by the nature of the surface. **The mobile crystal surface**
23 **influences the water monolayer dynamics, for which orientational and bonding characteristics**
24 **fluctuate rapidly. At a temperature of 300K, this leads to a weakly-bound first monolayer vis-à-**
25 **vis the static/fixed lattice.** The geometry of water molecules is similar to that reported by
26 quantum simulations [27]. For planar surfaces the second monolayer is further pushed thereby
27 affecting any stabilizing role played by secondary solvation of the charge transfer
28 products/adducts created at the first ML after photo-excitation of the crystal. It can be said that
29 rutile-(001) and anatase-(001) surfaces may play an important role by not hindering the removal
30 of products (H₂/O₂) formed at the first monolayer, which is a major problem with other surfaces
31
32
33
34
35
36
37
38
39
40
41
42
43
44
45
46
47
48
49
50
51
52
53
54
55
56
57
58
59
60

1
2
3 [30]. It has been shown that these interactions between the first and second monolayer through
4
5 hydrogen bonding depending on the rigidity of the first monolayer. Hopefully these simulations
6
7 will provide insights into modelling large scale simulations or macroscopic single crystal or an
8
9 ensemble of such particles in contact with water [31].
10
11

12 13 14 15 16 17 **Acknowledgements** 18

19 The authors acknowledge useful conversations with Dr. Damian Mooney. This material is based
20
21 upon works supported by the Science Foundation Ireland (SFI) under Grant No.
22
23 [07/SRC/B1160], in addition to the Irish Research Council for Science, Engineering and
24
25 Technology. We also thank SFI and the Irish Centre for High End Computing for the provision
26
27 of high performance computing facilities.
28
29
30
31
32
33
34
35
36
37
38
39
40
41
42
43
44
45
46
47
48
49
50
51
52
53
54
55
56
57
58
59
60

References

- [1] U. Diebold, *Surface Science Reports* **48** (5-8), 53 (2003)
- [2] A. Fujishima and K. Honda, *Nature* **238** (5358), 37 (1972)
- [3] J. W. Tang, J. R. Durrant, and D. R. Klug, *J. Am. Chem. Soc.* **130** (42), 13885 (2008)
- [4] F. A. Frame and F. E. Osterloh, *J. Phys. Chem. C* **114** (23), 10628
- [5] K. Maeda, N. Sakamoto, T. Ikeda et al., *Chem.-Eur. J.* **16** (26), 7750
- [6] K. Maeda, M. Higashi, D. L. Lu et al., *J. Am. Chem. Soc.* **132** (16), 5858
- [7] Y. H. Ng, A. Iwase, A. Kudo et al., *J. Phys. Chem. Lett.* **1** (17), 2607
- [8] M. W. Kanan and D. G. Nocera, *Science* **321** (5892), 1072 (2008)
- [9] A. Melis and T. Happe, *Plant Physiology* **127** (3), 740 (2001)
- [10] Kevin Sivula, Radek Zboril, Florian Le Formal et al., *J. Am. Chem. Soc.* **132** (21), 7436
- [11] O. Bikondoa, C. L. Pang, R. Ithnin et al., *Nature Materials* **5** (3), 189 (2006)
- [12] E. Wahlstrom, E. K. Vestergaard, R. Schaub et al., *Science* **303** (5657), 511 (2004); K. Onda, B. Li, J. Zhao et al., *Science* **308** (5725), 1154 (2005); R. Nakamura, T. Okamura, N. Ohashi et al., *J. Am. Chem. Soc.* **127** (37), 12975 (2005); F. Allegretti, S. O'Brien, M. Polcik et al., *Phys. Rev. Lett.* **95** (22), 4 (2005); I. M. Brookes, C. A. Muryn, and G. Thornton, *Phys. Rev. Lett.* **87** (26), 4 (2001)
- [13] Scott J. Thompson and Steven P. Lewis, *Physical Review B* **73** (7), 073403 (2006); M. L. Machesky, M. Predota, D. J. Wesolowski et al., *Langmuir* **24** (21), 12331 (2008); M. Machesky, M. Ridley, D. Wesolowski et al., *Geochimica Et Cosmochimica Acta* **71** (15), A609 (2007); L. Vlcek, Z. Zhang, M. L. Machesky et al., *Langmuir* **23** (9), 4925 (2007); N. Kumar, S. Neogi, P. R. C. Kent et al., *J. Phys. Chem. C* **113** (31), 13732 (2009)
- [14] A. V. Bandura and J. D. Kubicki, *J. Phys. Chem. B* **107** (40), 11072 (2003)
- [15] A. Valdes, Z. W. Qu, G. J. Kroes et al., *J. Phys. Chem. C* **112** (26), 9872 (2008)
- [16] P. Zarzycki, *J. Phys. Chem. C* **111** (21), 7692 (2007)
- [17] Philip J. D. Lindan, N. M. Harrison, and M. J. Gillan, *Phys. Rev. Lett.* **80** (4), 762 (1998)
- [18] E. Mamontov, L. Vlcek, D. J. Wesolowski et al., *J. Phys. Chem. C* **111** (11), 4328 (2007)
- [19] E. Mamontov, D. J. Wesolowski, L. Vlcek et al., *J. Phys. Chem. C* **112** (32), 12334 (2008)
- [20] M. Predota, A. V. Bandura, P. T. Cummings et al., *J. Phys. Chem. B* **108** (32), 12049 (2004)
- [21] W. Langel, *Surface Science* **496** (1-2), 141 (2002)
- [22] M. Leslie W. Smith, T.R. Forester, *The DL_POLY_2 User Manual*, edited by Editor v. 2.14 ed. (2003).
- [23] M. Matsui and M. Akaogi, *Mol. Sim.* **6**, 239 (1991)
- [24] Jacek. Goniakowski, Fabio. Finocchi, and Claudine. Noguera, *Reports on Progress in Physics* **71** (1), 016501 (2008)
- [25] Annabella Selloni, *Nature Materials* **7** (8), 613 (2008)
- [26] M. Sumita, C. P. Hu, and Y. Tateyama, *J. Phys. Chem. C* **114** (43), 18529 (2010)
- [27] G. Teobaldi, W. A. Hofer, O. Bikondoa et al., *Chemical Physics Letters* **437** (1-3), 73 (2007)
- [28] J. K. Gregory, D. C. Clary, K. Liu et al., *Science* **275** (5301), 814 (1997)
- [29] X. J. Han, L. Bergqvist, P. H. Dederichs et al., *Physical Review B* **81** (13) (2010)
- [30] L. M. Liu, P. Crawford, and P. Hu, *Progress in Surface Science* **84** (5-6), 155 (2009); D. Pillay, Y. Wang, and G. S. Hwang, *J. Am. Chem. Soc.* **128** (43), 14000 (2006)
- [31] A. S. Barnard, P. Zapol, and L. A. Curtiss, *Journal of Chemical Theory and Computation* **1** (1), 107 (2005)

Figure Captions

- 1
2
3
4
5 Fig. 1: Representative configurations of various rutile-water interfaces: (A) (110), (B) (100),
6 (C) (101), and (D) (001).
7
8
9 Fig. 2: Representative configurations of various anatase-water interfaces: (A) (101), and (B)
10 (001)
11
12
13 Fig. 3: Absolute density (gm cm^{-3}) of water above various planes of (a) rutile and (b) anatase.
14 The plane formed by the first surface titanium atoms was used for projection of the
15 vectors (see text for details).
16
17
18
19 Fig. 4: Probability distribution of the water $\text{H}_w\text{-O}_w\text{-H}_w$ angle in the adsorbed monolayer in
20 contact with each surface.
21
22
23 Fig. 5: Distribution of the water $\text{O}_w\text{-H}_w$ bond length in the adsorbed monolayer in contact with
24 each surface.
25
26
27 Fig. 6: Distribution of the water absolute dipole moment in the adsorbed monolayer in contact
28 with each surface.
29
30
31 Fig. 7: Distribution of the cosine of angle of the monolayer's water molecules' dipole vectors
32 with respect to the plane of the crystal surfaces, θ , for various faces of (a) rutile, and (b)
33 anatase. A cosine of zero indicates dipole alignment normal to the face, while ± 1
34 indicates parallel dipole alignment, oriented parallel, or along, the surface.
35
36
37
38
39 Fig. 8: Distribution of the cosine of angle of the first two layers of water molecules' dipole
40 vectors with respect to the plane of the crystal surfaces, θ , for various faces: (A) Rutile
41 (110), (B) Rutile (100), (C) Rutile (101), (D) Rutile (001), (E) Anatase (101), (F)
42 Anatase (001). A cosine of zero indicates dipole alignment normal to the face, while ± 1
43 indicates parallel dipole alignment, oriented parallel, or along, the surface.
44
45
46
47
48
49
50
51
52
53
54
55
56
57
58
59
60

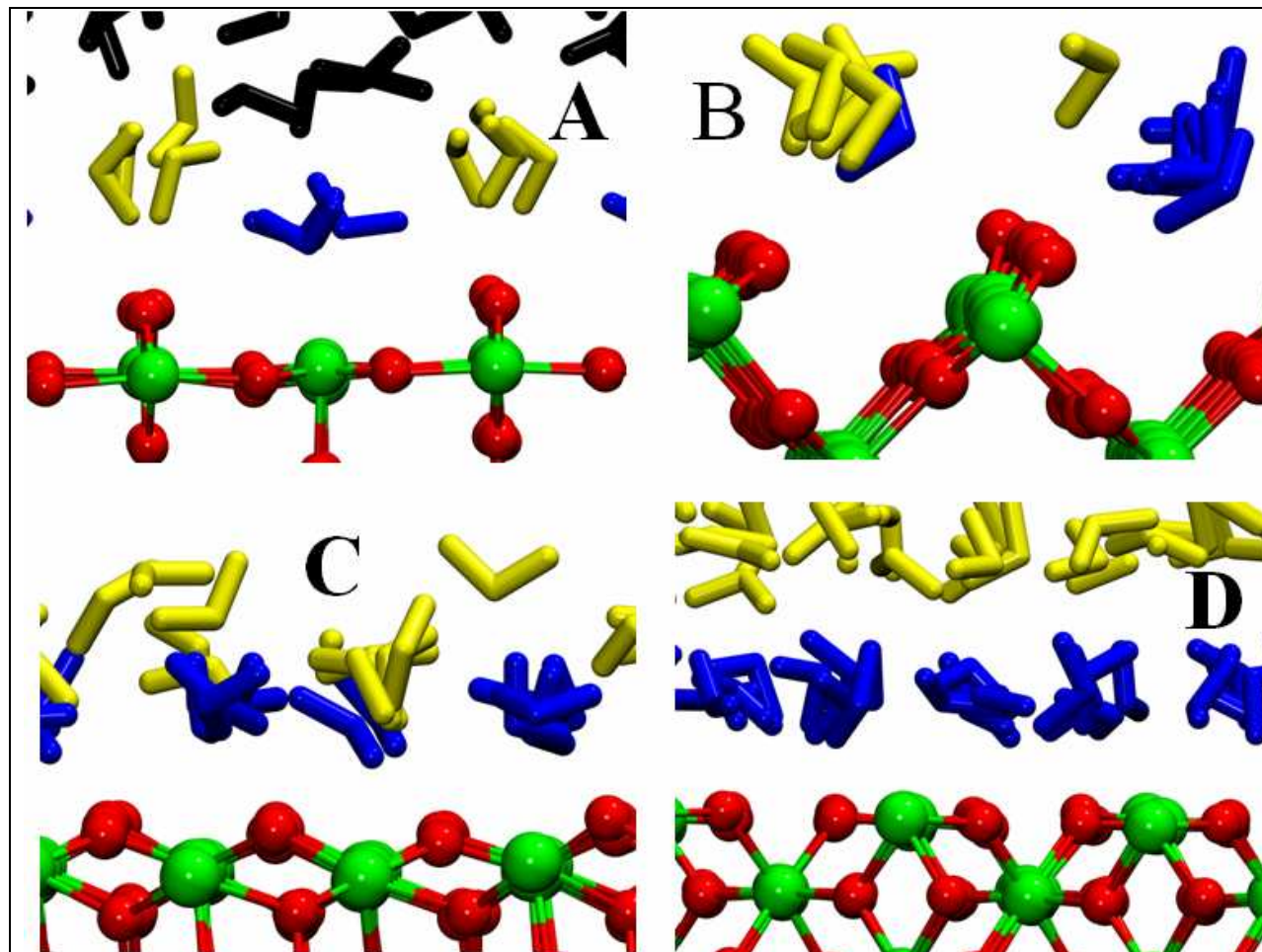


Fig. 1: Representative configurations of various rutile-water interfaces: (A) (110), (B) (100), (C) (101), and (D) (001). (blue- 1 ML, yellow- 2 ML)

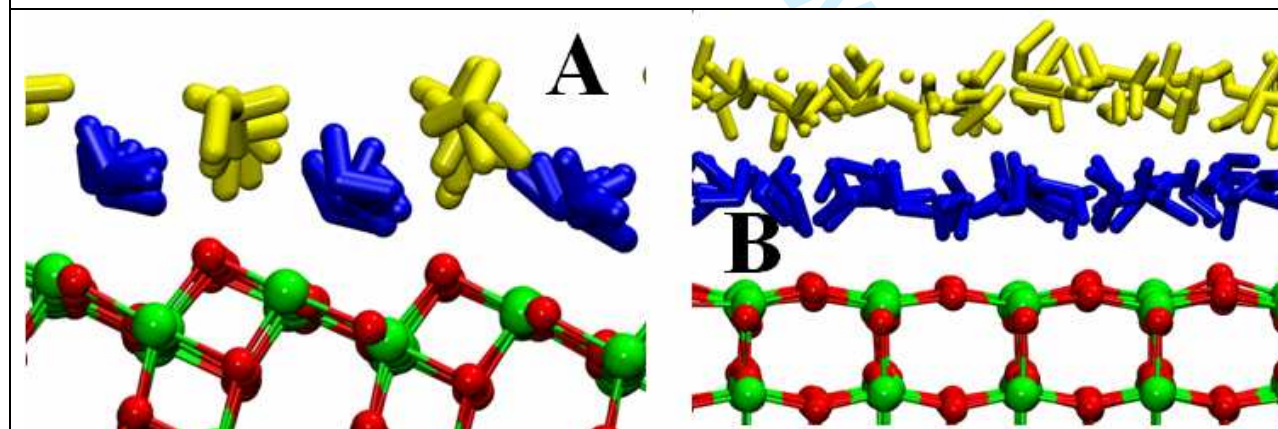


Fig. 2: Representative configurations of various anatase-water interfaces: (A) (101), and (B) (001) (blue- 1 ML, yellow- 2 ML)

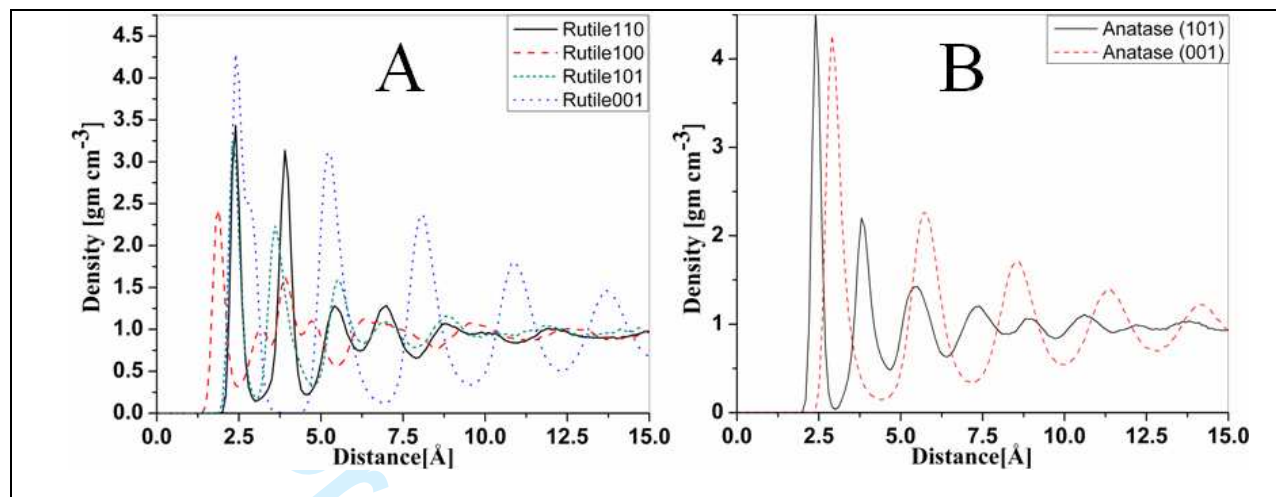


Fig 3: Absolute density (gm cm^{-3}) of water above various planes of (a) rutile and (b) anatase. The plane formed by the first surface titanium atoms was used for projection of the vectors (see text for details).

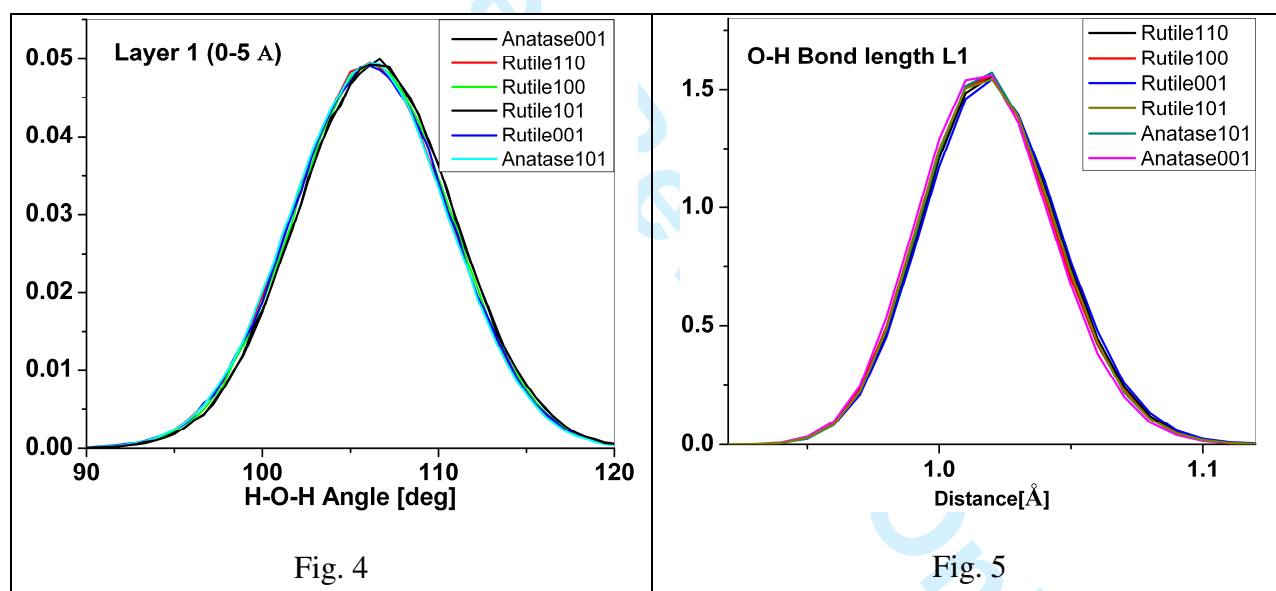


Fig. 4: Probability distribution of the water H-O-H angle in the adsorbed L1 (0-5 \AA) in contact with each surface

Fig. 5: Distribution of the water O-H bond length in the adsorbed monolayer in contact with each surface

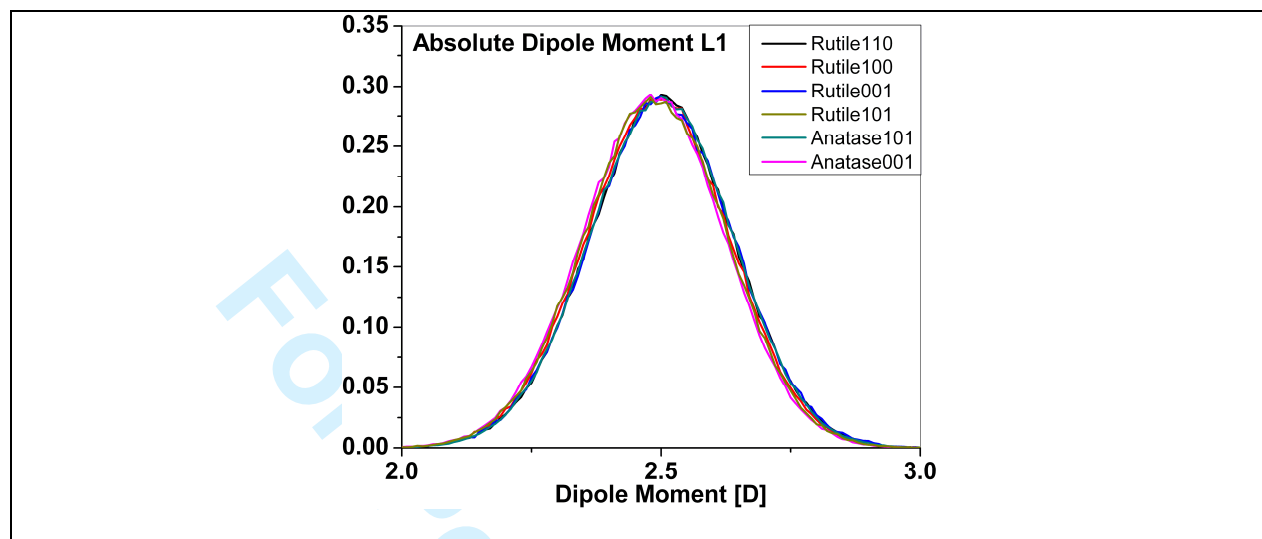


Fig. 6: Distribution of the water absolute dipole moment within 0 to 5 Å from the surface.

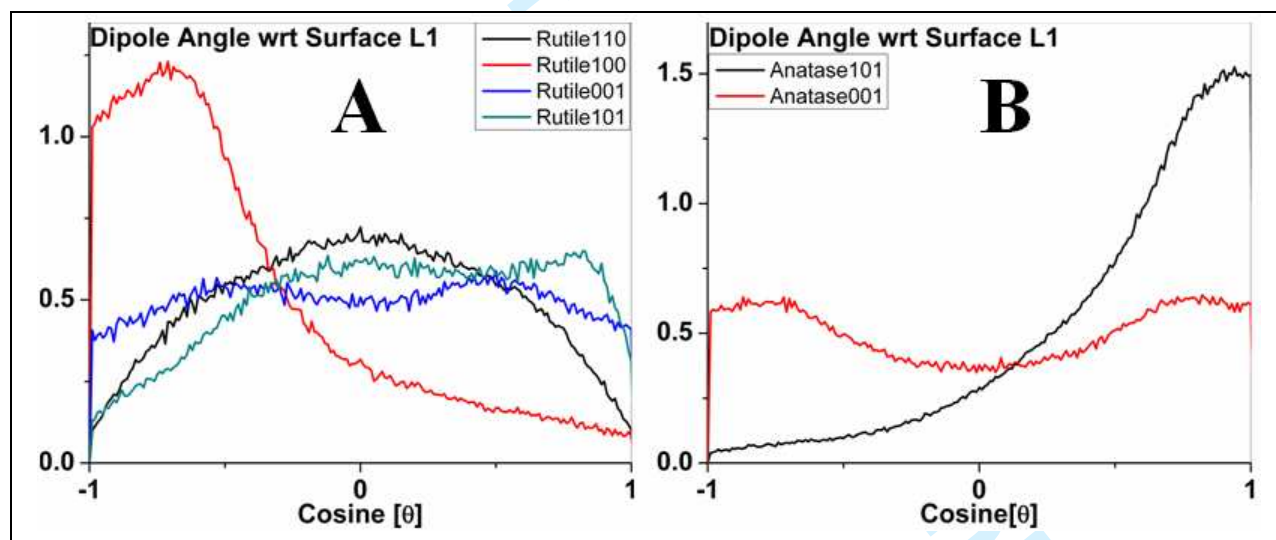


Fig. 7: Distribution of the cosine of angle of water molecules' dipole vectors with respect to the plane of the crystal surfaces, θ , within 5 Å from the surface for various faces of (a) rutile, and (b) anatase. A cosine of zero indicates dipole alignment normal to the face, while ± 1 indicates parallel dipole alignment, oriented parallel, or along, the surface.

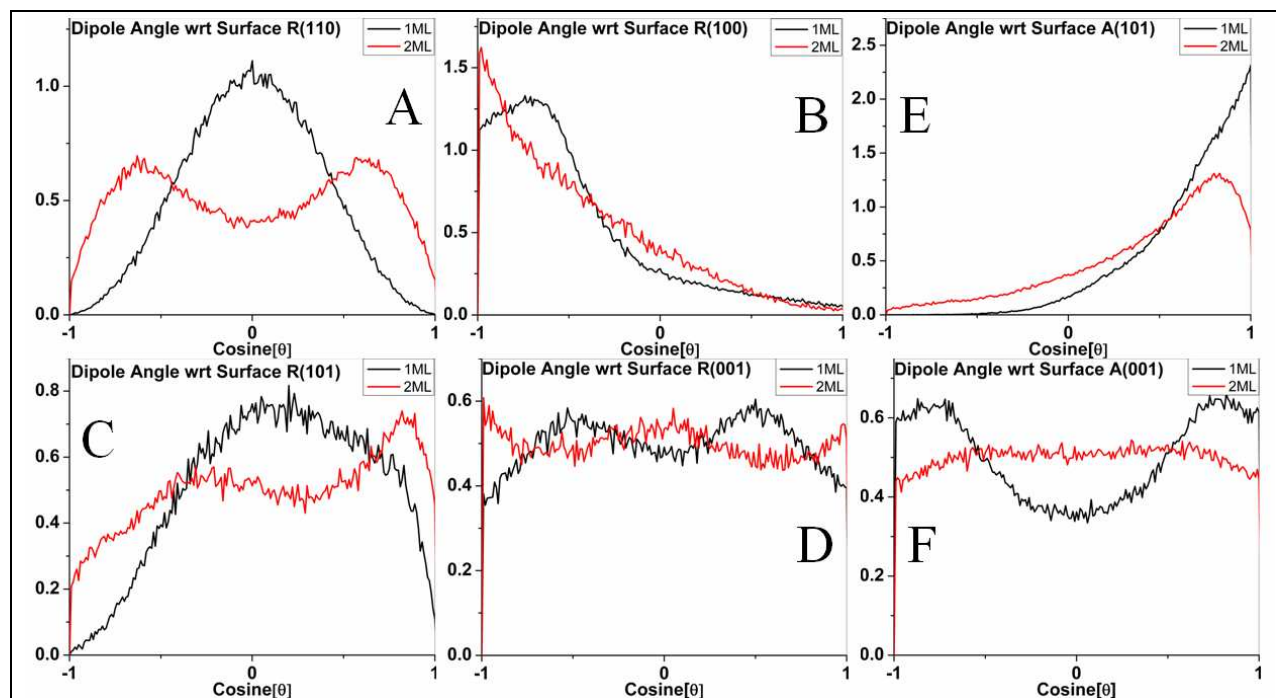


Fig. 8: Distribution of the cosine of angle of the first two layers of water molecules' dipole vectors with respect to the plane of the crystal surfaces, θ , for various faces: (A) Rutile (110), (B) Rutile (100), (C) Rutile (101), (D) Rutile (001), (E) Anatase (101), (F) Anatase (001). A cosine of zero indicates dipole alignment normal to the face, while ± 1 indicates parallel dipole alignment, oriented parallel, or along, the surface.

Phase (surface), X, Y, Z (Å)	System Size
Rutile (110) 26.26, 45.47, 69.490	(TiO ₂) ₆₃₀ (H ₂ O) ₂₀₀₀
Rutile(100) 22.97, 26.63, 70.00	(TiO ₂) ₄₀₅ (H ₂ O) ₉₅₀
Rutile(101) 27.33, 27.56, 113.47	(TiO ₂) ₃₀₀ (H ₂ O) ₂₄₆₈
Rutile(001) 22.97, 22.97, 124.00	(TiO ₂) ₄₀₀ (H ₂ O) ₁₇₂₀
Anatase(101) 71.46, 26.43, 72.680	(TiO ₂) ₁₁₇₆ (H ₂ O) ₃₁₆₂
Anatase(001) 33.98, 33.98, 124.00	(TiO ₂) ₆₄₈ (H ₂ O) ₃₉₀₀

Table I: Details of geometries used

<i>Buckingham potential for TiO₂ and water oxygen: $A_{ij} \times \exp(-r_{ij}/\rho_{ij}) - C_{ij}/r_{ij}^6$</i>			
<i>i - j</i>	<i>A_{ij}</i> (kcal mol ⁻¹)	<i>ρ_{ij}</i> (Å)	<i>C_{ij}</i> (kcal mol ⁻¹ Å ⁶)
Ti - O	391049.1	0.194	290.331
Ti - Ti	717647.4	0.154	121.067
O - O	271716.3	0.234	696.888
Ti - O _w	28593.0	0.265	148.000
<i>Lennard-Jones potential for water: $(q_i q_j / r_{ij}) + \epsilon_{ij} [(\sigma_{ij}/r_{ij})^{12} - (\sigma_{ij}/r_{ij})^6]$</i>			
<i>i - j</i>	<i>ε_{ij}</i> (kcal mol ⁻¹)	<i>σ_{ij}</i> (Å)	
O _w - O _w	0.15539	3.5532	
<i>Morse bond potential for water: $A_{ij} [1 - \exp(-k_{ij}(r_{ij} - r_{ij}^0))]^2 - A_{ij}$</i>			
<i>i - j</i>	<i>A_{ij}</i> (kcal mol ⁻¹)	<i>k_{ij}</i> (Å ⁻¹)	<i>r_{ij}⁰</i> (Å)
O _w - H _w	101.905	2.347	1.00
<i>Harmonic angle bending potential for water: $k/2 \times (\theta - \theta_0)$</i>			
<i>i - j - k</i>	<i>θ₀</i> deg	<i>k</i> (kcal mol ⁻¹ rad ⁻²)	
H - O - H	109.47	103.045	
Atomic charges: q(Ti) = 2.196 e, q(O) = -1.098 e, q(O _w) = -0.82 e, q(H _w) = 0.41 e; O _w , H _w = water oxygen and hydrogen atoms			
Table II: Force field parameters			

Figure Captions

Cover Page: Representative figure of sampled regions of water above the surface of TiO₂-Rutile (110) face.

Fig. 1: Representative configurations of various rutile-water interfaces: (A) (110), (B) (100), (C) (101), and (D) (001).

Fig. 2: Representative configurations of various anatase-water interfaces: (A) (101), and (B) (001)

Fig. 3: Absolute density (gm cm⁻³) of water above various planes of (a) rutile and (b) anatase. The plane formed by the first surface titanium atoms was used for projection of the vectors (see text for details).

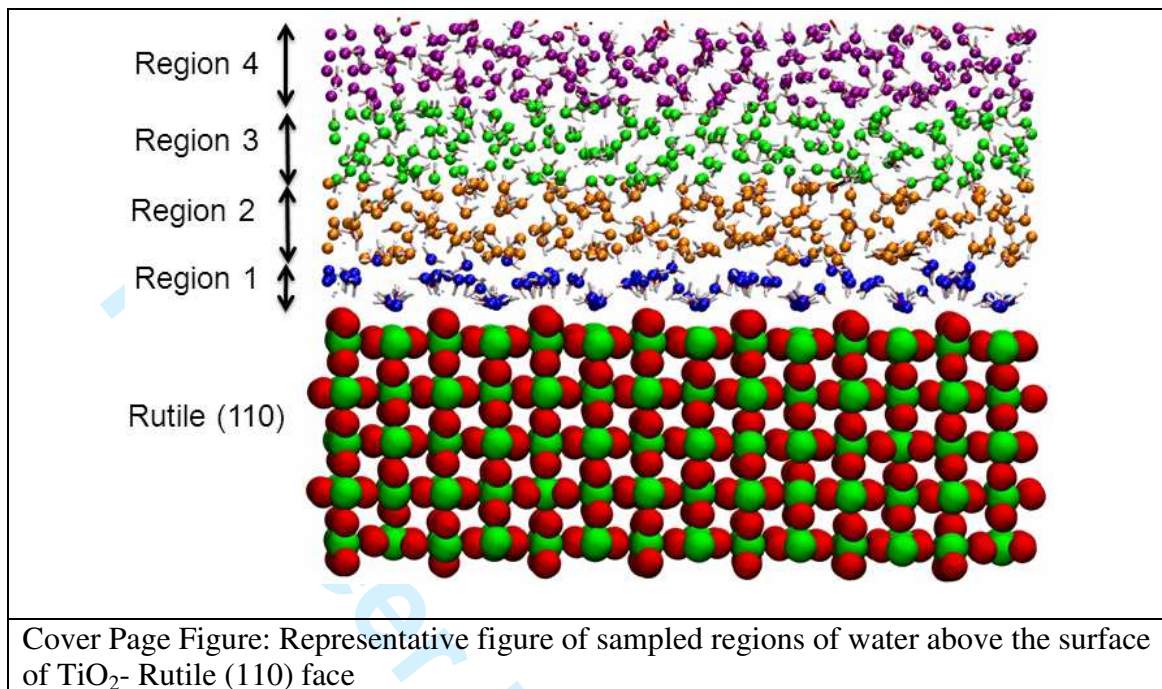
Fig. 4: Probability distribution of the water H_w-O_w-H_w angle in the adsorbed monolayer in contact with each surface.

Fig. 5: Distribution of the water O_w-H_w bond length in the adsorbed monolayer in contact with each surface.

Fig. 6: Distribution of the water absolute dipole moment in the adsorbed monolayer in contact with each surface.

Fig. 7: Distribution of the cosine of angle of the monolayer's water molecules' dipole vectors with respect to the plane of the crystal surfaces, θ , for various faces of (a) rutile, and (b) anatase. A cosine of zero indicates dipole alignment normal to the face, while ± 1 indicates parallel dipole alignment, oriented parallel, or along, the surface.

Fig. 8: Distribution of the cosine of angle of the first two layers of water molecules' dipole vectors with respect to the plane of the crystal surfaces, θ , for various faces: (A) Rutile (110), (B) Rutile (100), (C) Rutile (101), (D) Rutile (001), (E) Anatase (101), (F) Anatase (001). A cosine of zero indicates dipole alignment normal to the face, while ± 1 indicates parallel dipole alignment, oriented parallel, or along, the surface.



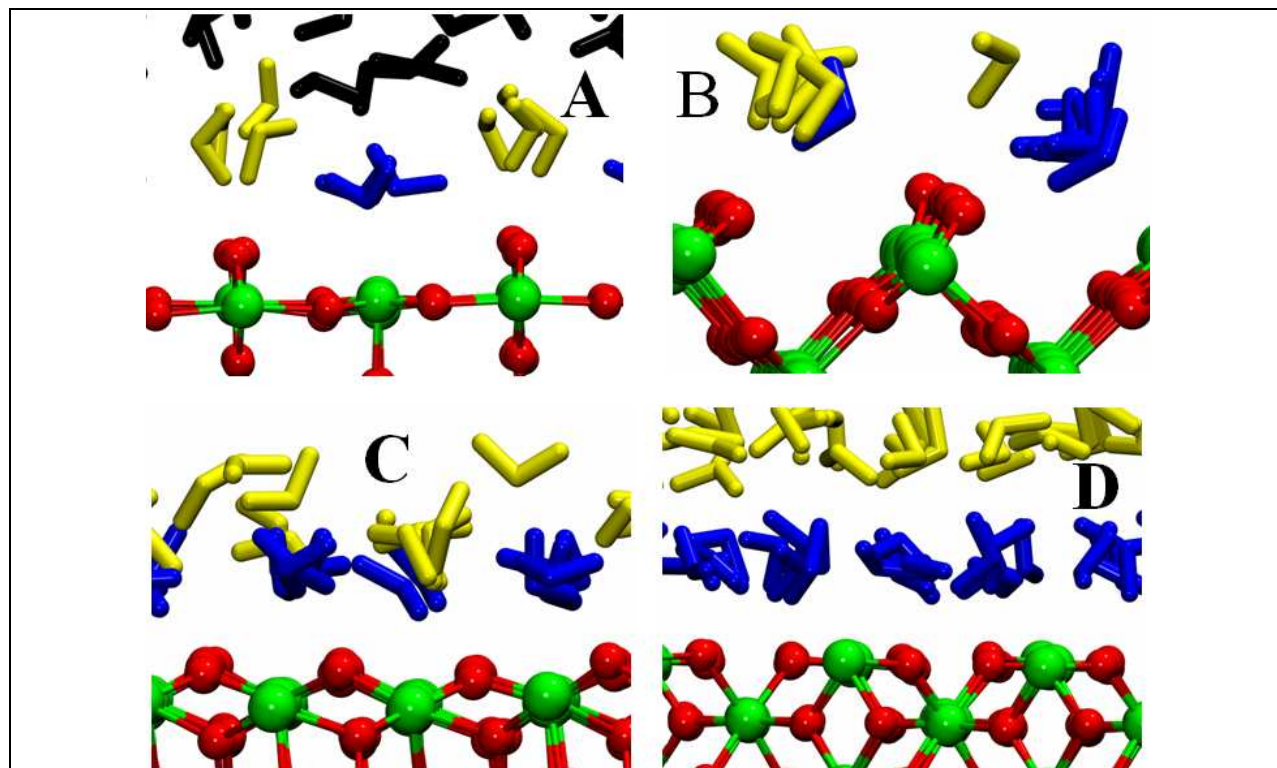


Fig. 1: Representative configurations of various rutile-water interfaces: (A) (110), (B) (100), (C) (101), and (D) (001). (blue- 1 ML, yellow- 2 ML)

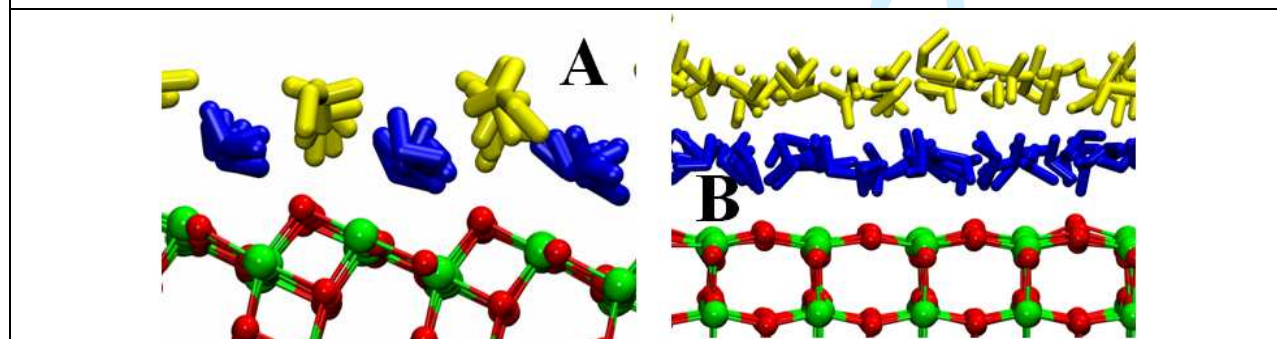


Fig. 2: Representative configurations of various anatase-water interfaces: (A) (101), and (B) (001) (blue- 1 ML, yellow- 2 ML)

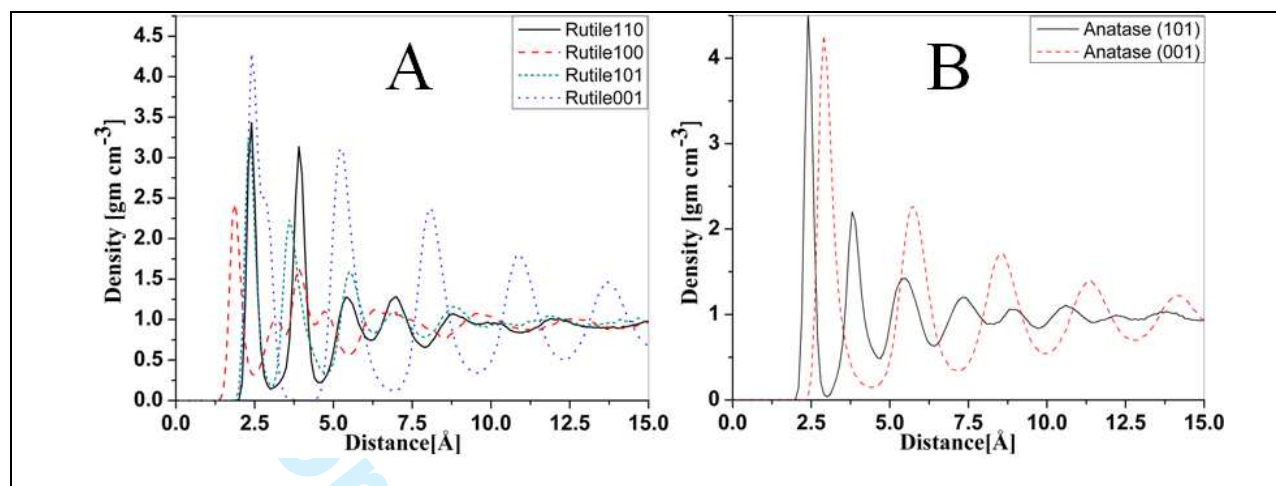


Fig 3: Absolute density (gm cm^{-3}) of water above various planes of (a) rutile and (b) anatase. The plane formed by the first surface titanium atoms was used for projection of the vectors (see text for details).

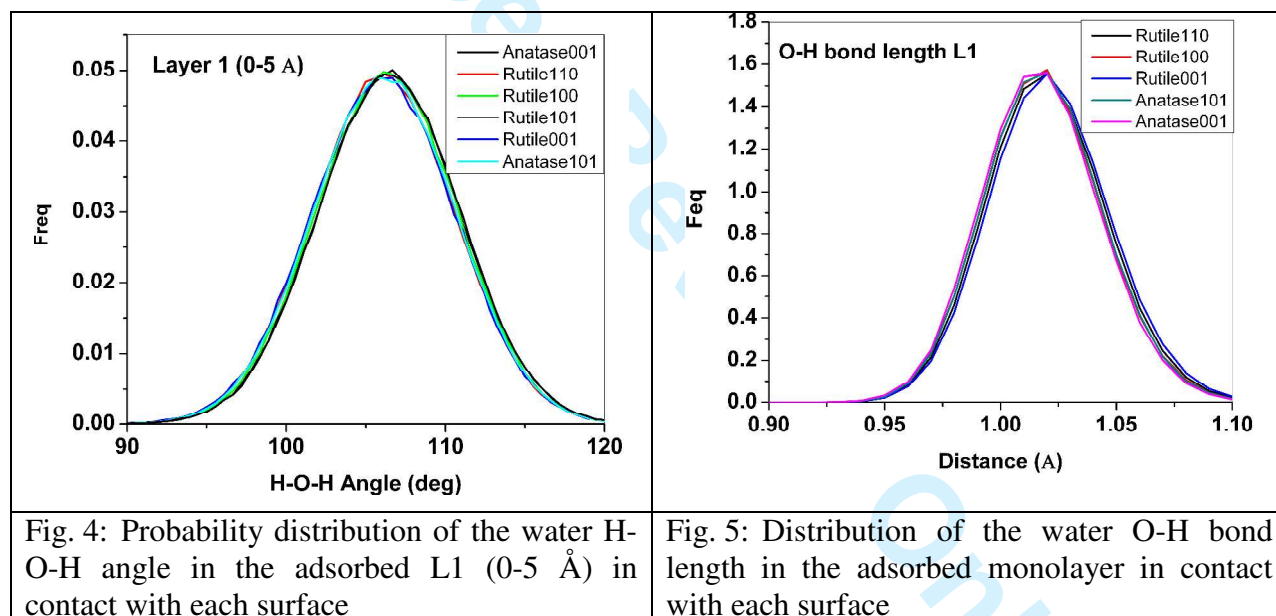
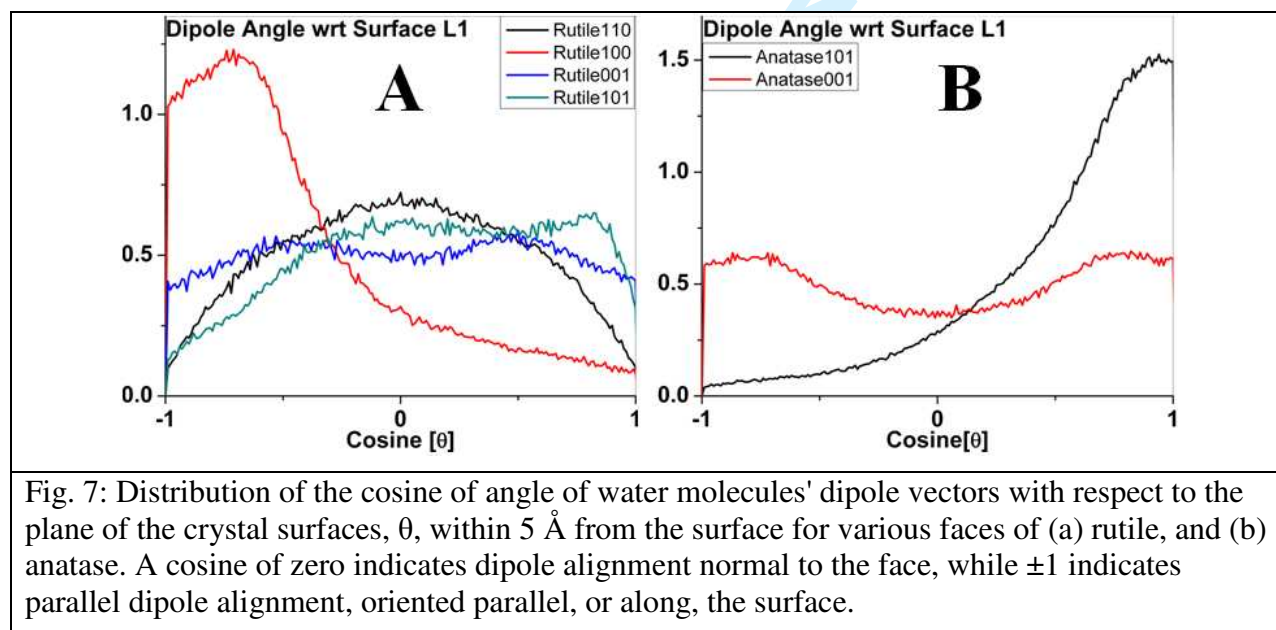
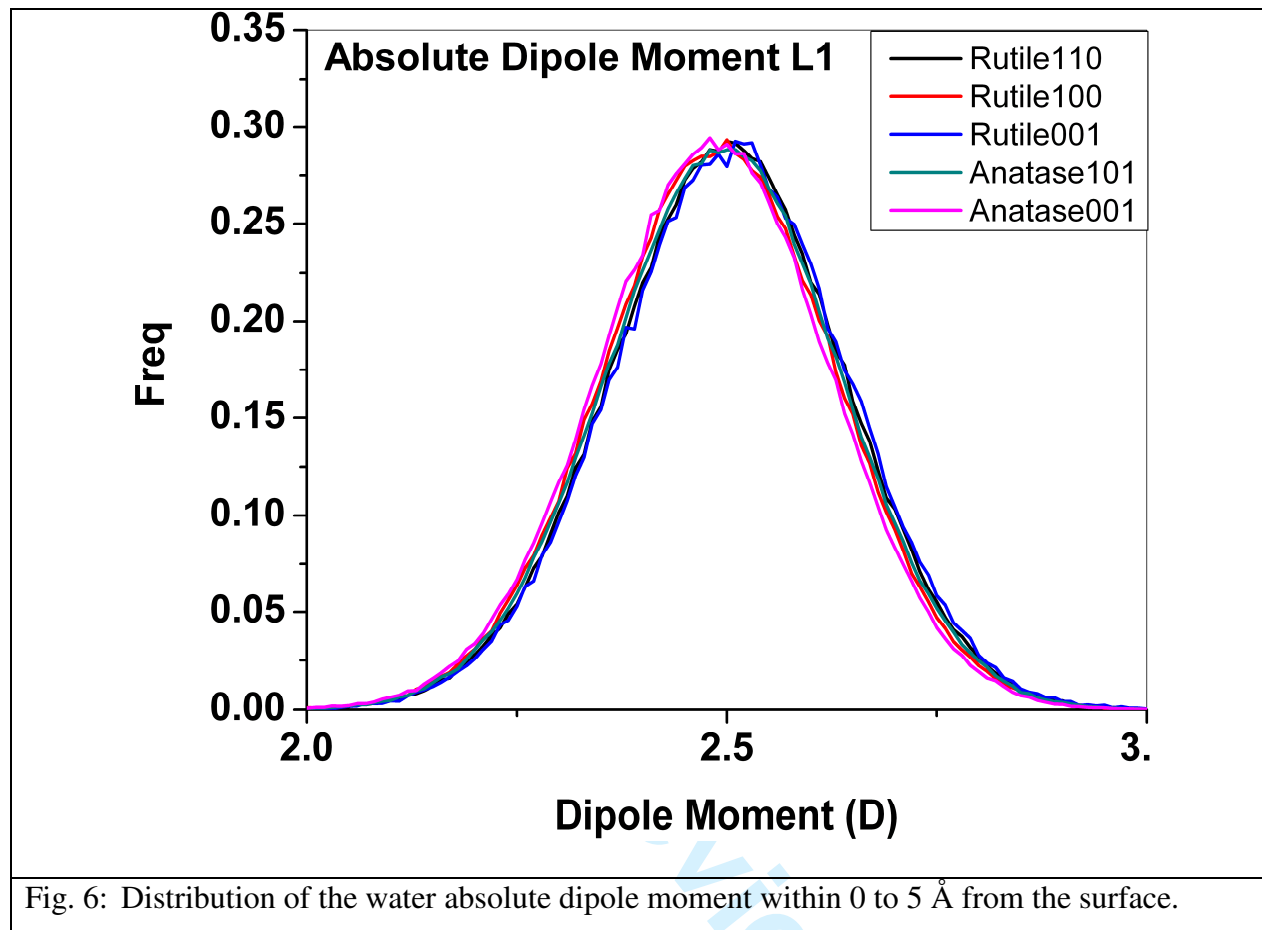


Fig. 4: Probability distribution of the water H-O-H angle in the adsorbed L1 (0-5 \AA) in contact with each surface

Fig. 5: Distribution of the water O-H bond length in the adsorbed monolayer in contact with each surface



53
54
55
56
57
58
59
60

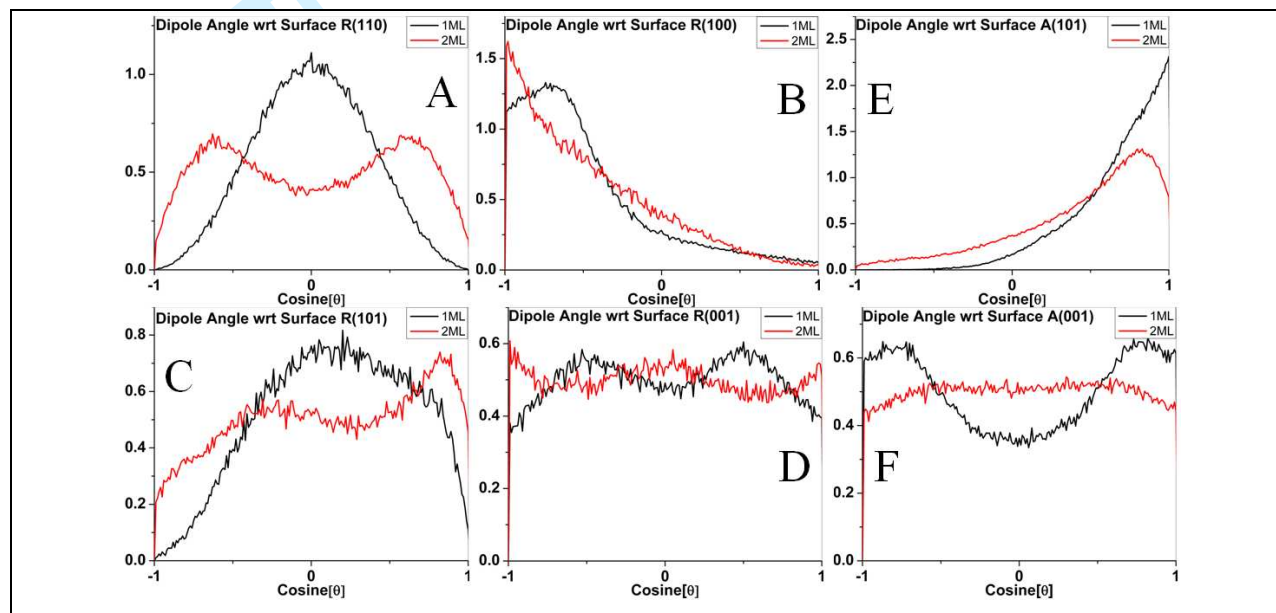


Fig. 8: Distribution of the cosine of angle of the first two layers of water molecules' dipole vectors with respect to the plane of the crystal surfaces, θ , for various faces: (A) Rutile (110), (B) Rutile (100), (C) Rutile (101), (D) Rutile (001), (E) Anatase (101), (F) Anatase (001). A cosine of zero indicates dipole alignment normal to the face, while ± 1 indicates parallel dipole alignment, oriented parallel, or along, the surface.

Phase (surface), X, Y, Z (Å)	System Size
Rutile (110) 26.26, 45.47, 69.490	(TiO ₂) ₆₃₀ (H ₂ O) ₂₀₀₀
Rutile(100) 22.97, 26.63, 70.00	(TiO ₂) ₄₀₅ (H ₂ O) ₉₅₀
Rutile(101) 27.33, 27.56, 113.47	(TiO ₂) ₃₀₀ (H ₂ O) ₂₄₆₈
Rutile(001) 22.97, 22.97, 124.00	(TiO ₂) ₄₀₀ (H ₂ O) ₁₇₂₀
Anatase(101) 71.46, 26.43, 72.680	(TiO ₂) ₁₁₇₆ (H ₂ O) ₃₁₆₂
Anatase(001) 33.98, 33.98, 124.00	(TiO ₂) ₆₄₈ (H ₂ O) ₃₉₀₀

Table I: Details of geometries used

<i>Buckingham potential for TiO₂ and water oxygen: $A_{ij} \times \exp(-r_{ij}/\rho_{ij}) - C_{ij}/r_{ij}^6$</i>			
i - j	A _{ij} (kcal mol ⁻¹)	ρ _{ij} (Å)	C _{ij} (kcal mol ⁻¹ Å ⁶)
Ti - O	391049.1	0.194	290.331
Ti - Ti	717647.4	0.154	121.067
O - O	271716.3	0.234	696.888
Ti - O _w	28593.0	0.265	148.000
<i>Lennard-Jones potential for water: $(q_i q_j / r_{ij}) + \epsilon_{ij} [(\sigma_{ij}/r_{ij})^{12} - (\sigma_{ij}/r_{ij})^6]$</i>			
i - j	ε _{ij} (kcal mol ⁻¹)	σ _{ij} (Å)	
O _w - O _w	0.15539	3.5532	
<i>Morse bond potential for water: $A_{ij} [1 - \exp(-k_{ij}(r_{ij} - r_{ij}^0))]^2 - A_{ij}$</i>			
i - j	A _{ij} (kcal mol ⁻¹)	k _{ij} (Å ⁻¹)	r _{ij} ⁰ (Å)
O _w - H _w	101.905	2.347	1.00
<i>Harmonic angle bending potential for water: $k/2 \times (\theta - \theta_0)$</i>			
i - j - k	θ ₀ deg	k (kcal mol ⁻¹ rad ⁻²)	
H - O - H	109.47	103.045	
Atomic charges: q(Ti) = 2.196 e, q(O) = -1.098 e, q(O _w) = -0.82 e, q(H _w) = 0.41 e; O _w , H _w = water oxygen and hydrogen atoms			

Table II: Force field parameters